

## X-ray magnetic circular dichroism and cluster-model analysis of the spinel-type oxide $\text{CoV}_2\text{O}_4$

Yosuke Nonaka<sup>1,\*</sup>, Goro Shibata<sup>1</sup>, Rui Koborinai<sup>2</sup>, Keisuke Ishigami<sup>1</sup>, Shoya Sakamoto<sup>1</sup>, Keisuke Ikeda<sup>1</sup>, Zhendong Chi<sup>1</sup>, Arata Tanaka<sup>3</sup>, Tsuneharu Koide<sup>4</sup>, Takuro Katsufuji<sup>2,5</sup>, Atsushi Fujimori<sup>1</sup>

<sup>1</sup>Department of Physics, University of Tokyo, Tokyo 113-0033 Japan

<sup>2</sup>Department of Physics, Waseda University, Tokyo 169-8555, Japan

<sup>3</sup>Department of Quantum Matter, ADSM, Hiroshima University, Higashi-Hiroshima 739-8530, Japan

<sup>4</sup>Photon Factory, Tsukuba 305-0801, Japan

<sup>5</sup>Kagami Memorial Laboratory for Material Science and Technology, Waseda University, Tokyo 169-0051, Japan

### 1 Introduction

Spinel-type transition metal oxides  $AB_2O_4$  are one of the most attractive playgrounds for the studies of emergent physical properties arising from frustrations in strongly correlated electron systems. Geometrical spin frustration exists in the pyrochlore (diamond) sublattice consisting of the B (A) sites as shown in Fig. 1 (b). In addition to spin frustration, orbital frustration (orbital degree of freedom) also exists in the triply degenerated V  $t_{2g}$  orbitals of the spinel-type vanadates  $AV_2O_4$  as shown in Fig. 1 (c). This system is suitable for detailed studies of orbital states and their relationship to lattice distortion because of the absence of complicated structural distortions such as the  $\text{GdFeO}_3$ -type distortion in perovskite-type oxides. Thus, many theoretical and experimental studies have been performed on spinel-type vanadates [1], particularly, on orbital ordering in  $AV_2O_4$  (A = Zn, Mn, Fe, Cd...). Moreover, recently orbital glass (short-range orbital ordering) state was found in  $\text{CoV}_2\text{O}_4$  [2, 3]. In the present study, we have studied the spin and orbital states of  $\text{CoV}_2\text{O}_4$  using x-ray absorption spectroscopy (XAS) and x-ray magnetic circular dichroism (XMCD) and subsequent configuration-interaction (CI) cluster-model analysis.

### 2 Experiment

Bulk single crystals of  $\text{CoV}_2\text{O}_4$  were grown by the floating zone method. In order to avoid the formation of the  $\text{V}_2\text{O}_3$  impurity phase, the compositions of the feed rod was not stoichiometric (Co : V = 1 : 2) but containing 50% excess Co relative to the stoichiometric one (Co : V = 1.5 : 2). The Co : V ratio of the synthesized single crystals was estimated to be 1.21 : 1.79 by induction-coupled plasma analysis.

The XAS and XMCD measurements at the Co and V  $L_{2,3}$  edges were performed at BL-16A of Photon Factory. The spectra were taken in the total electron yield mode at 30, 70, and 90 K. Figure 2 shows experimental geometry. The sample angle was fixed so that the incident x-rays form an angle of 45 degree from the [110] direction and within the [001]-[110] plane. The magnetic field of 0.5 T was applied along the [001] and [111] directions using an ‘vector magnet’ XMCD apparatus [4]. In order to obtain

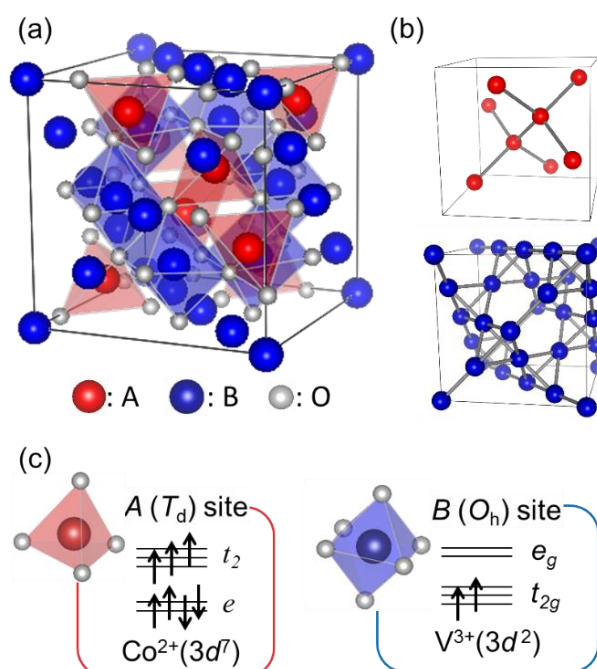


Fig. 1: Illustrations of the crystal structure and the electronic configurations of the 3d orbitals of the spinel-type oxide. (a) Cubic unit cell of  $AB_2O_4$ . The red (blue) polyhedra denotes the  $\text{AO}_4$  tetrahedra ( $\text{BO}_6$  octahedra). (b) Pyrochlore and diamond structure consisting of B (A) site network. (c) Electronic configurations of the  $\text{Co}^{2+}$  ( $\text{V}^{3+}$ ) ion at the tetrahedral (octahedral) site.

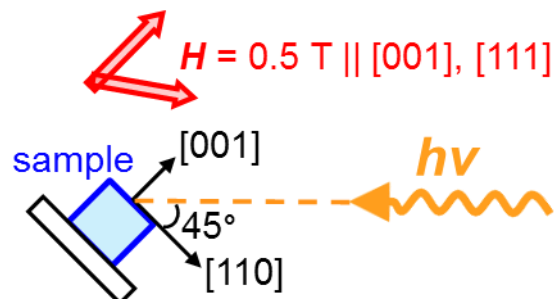


Fig. 2: Schematic picture of the experimental geometry.

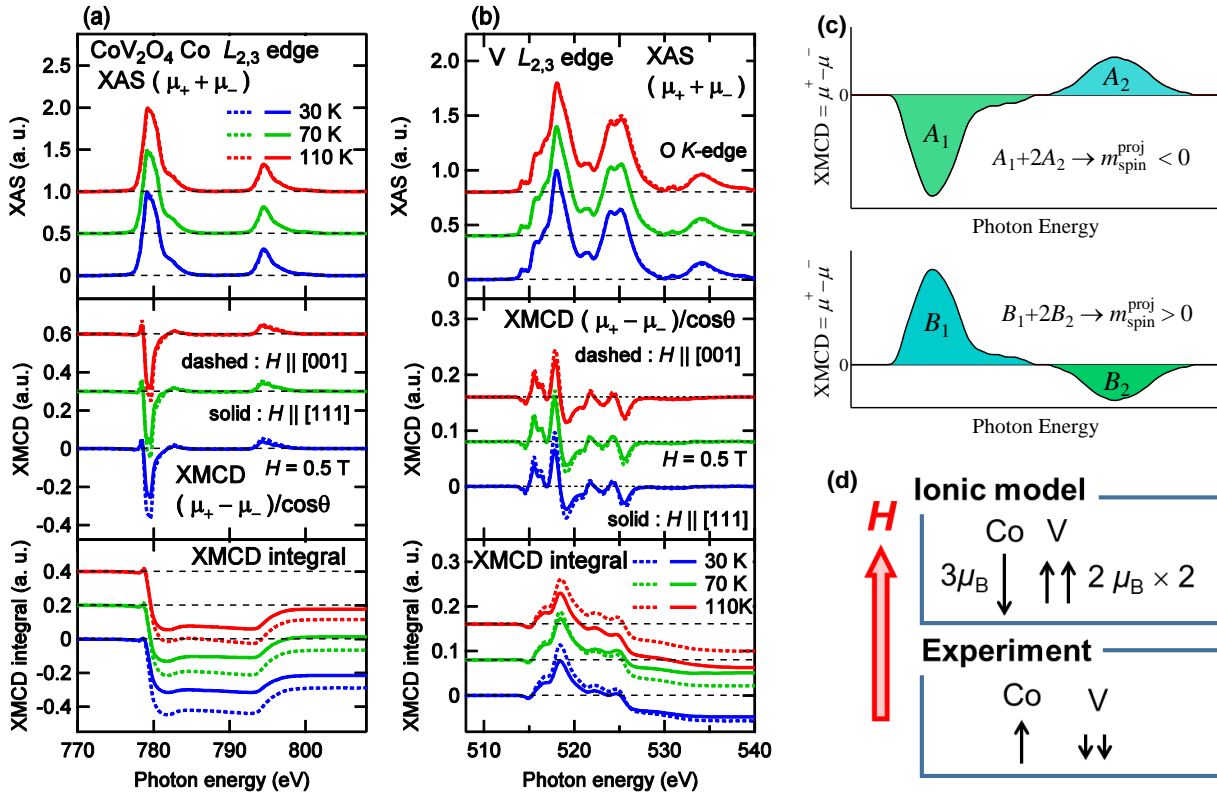


Fig. 3: Experimental spectra and the spin configurations for  $\text{CoV}_2\text{O}_4$ . (a, b) XAS, XMCD, and XMCD integral spectra at (a) Co  $L_{2,3}$  and (b) V  $L_{2,3}$  edges under the magnetic field of 0.5 T along the [001] and [111] directions. (c) Schematic XMCD spectra corresponding to positive (upper panel) and negative (lower panel) directions of spin magnetic moment. (d) Directions of spin magnetic moment expected from the ionic model and those indicated by experiment.

clean surfaces, the samples were fractured in the ultra-high vacuum of the apparatus.

### 3 Results and Discussion

Figures 3 (a) and (b) show the XAS and XMCD spectra of  $\text{CoV}_2\text{O}_4$ . As shown in the Fig. 3 (c) the sign of the XMCD spectrum at the  $L_3$  and  $L_2$  edges indicate whether the projection of the spin magnetic moment onto the X-ray incident vector  $m_{\text{spin}}^{\text{proj}}$  is positive or negative. In the ionic picture shown in Fig. 1 (c), the total spin magnetic moment of the two  $\text{V}^{3+}$  ( $2\mu_B \times 2$  ions =  $4\mu_B$ ) ions is larger than that of the  $\text{Co}^{2+}$  ( $3\mu_B$ ) ion and, therefore, the spin magnetic moment of the  $\text{V}^{3+}$  ion is expected to be parallel to the applied magnetic fields as shown in the upper panel of Fig. 3 (d). However, the signs of these XMCD signals in the middle panels of Fig. 3 (a) and (b) show that the magnetic moments of Co ion are aligned parallel to the magnetic field and that those of V ion are anti-parallel to it as shown in the lower panel of Figs. 3 (d).

In order to take the excess Co atoms into account, we have fitted the experimental spectra at the Co  $L_{2,3}$  edge to the sum of calculated spectra for the tetrahedral and octahedral sites. Since the Co : V ratio of this sample was estimated to 1.21 : 1.79,  $\text{V}^{3+}$  ions at octahedral site might be replaced by the excess  $\text{Co}^{3+}$  ions. CI cluster-model calculation has been performed for the tetrahedral site

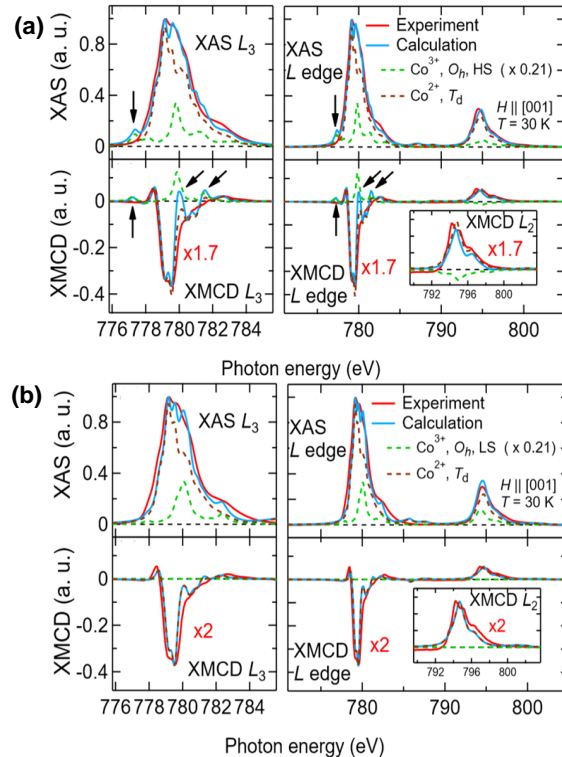


Fig. 4: Comparison between calculated spectra and experiment. The spectra of excess Co are assumed to be (a) HS and (b) LS state. Discrepancies between the calculation and experiment are marked by black arrows.

Table 1: The values of parameters used for the CI cluster-model and the multiplet calculations.

	Parameters used for the calculations (eV)					
	Tetrahedral site				Octahedral site	
	$\Delta$	$pd\sigma$	$10Dq$	$U_{dd}$	$10Dq$	$\Delta E$
Co <sup>2+</sup> ( $T_d$ ) with excess Co <sup>3+</sup> (HS, $O_h$ )	6.5	1.8	-0.3 (fixed)	5.0 (fixed)	1.9 (fixed)	+0.20
Co <sup>2+</sup> ( $T_d$ ) with excess Co <sup>3+</sup> (LS, $O_h$ )	4.5	1.7	-0.3 (fixed)	5.0 (fixed)	2.5 (fixed)	-0.25

(the main component), whereas atomic multiplet calculation has been adopted for the octahedral site (excess Co, the minor component) in order to reduce the number of adjustable parameters. The ratio of the Co<sup>2+</sup> at tetrahedral site and the Co<sup>3+</sup> at octahedral site have been set as Co<sup>2+</sup> ( $T_d$ ) : Co<sup>3+</sup> ( $O_h$ ) = 1 : 0.21. The crystal-field splitting  $10Dq$  of the octahedral site has been set to 2.5 eV and 1.9 eV in order to simulate the Co<sup>3+</sup> low-spin (LS) and high-spin (HS) states, respectively.  $10Dq$  and the intra-atomic  $3d-3d$  coulomb energy  $U_{dd}$  at the tetrahedral site have been assumed to be -0.3 eV and 5.0 eV, respectively, and the charge-transfer energy  $\Delta$  and the Slater-Koster parameter  $pd\sigma$  for the tetrahedral site, and the energy shift of the octahedral spectra  $\Delta E$  have been taken as adjustable parameters.

Figures 4 (a) and (b) show the result of fitting assuming the HS and LS state for the excess Co in octahedral site, respectively. In Fig. 4 (a), discrepancies between the calculation and experiment are marked by black arrows. In contrast, Fig. 4 (b) shows good agreement between calculation and experiment. These results indicate that the LS state is more likely for the excess Co. The parameters used for the calculations are listed in Table 1.

Figures 5 show the spin and orbital magnetic moments obtained using the XMCD sum rules [4, 5]. Since the excess Co ions take the trivalent LS state at the octahedral site, we have subtracted the contribution of the excess Co ions from the XAS. The orbital magnetic moment of V is almost quenched ( $\leq 0.1 \mu_B$ ) even below 90 K, at which a transition temperature to the orbital glass state has been reported [2]. Therefore, the almost quenched orbital magnetic moment indicates that the short-range ordered orbitals are predominantly real number and not complex.

#### References

- [1] S. -H. Lee, H. Takagi, D. Louca, M. Matsuda, S. Ji, H. Ueda, Y. Ueda, T. Katsufuji, J. -H. Chung, S. Park, S. -W. Cheong, and C. Broholm., *J. Phys. Soc. Jpn.* **65**, 1053 (1996).
- [2] R. Koborinai, S. E. Dissanayake, M. Reehuis, M. Matsuda, T. Kajita, H. Kuwahara, S.-H. Lee, and T. Katsufuji, *Phys. Rev. Lett.* **116**, 037201 (2016).
- [3] D. Reig-i-Plessis, D. Casavant, V. O. Garlea, A. A. Aczel, M. Feyngenson, J. Neuefeind, H. D. Zhou, S. E. Nagler, and G. J. MacDougall, *Phys. Rev. B* **93**, 014437 (2016).

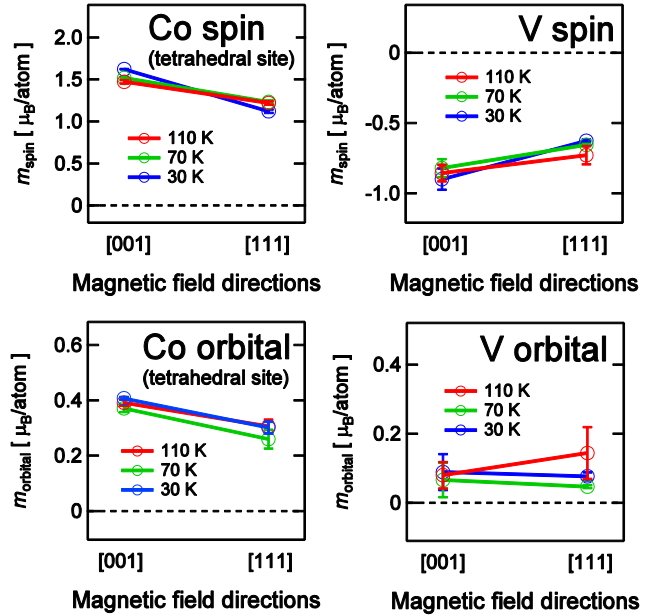


Fig. 5: Spin and orbital magnetic moments of the Co and V ion under the magnetic field of 0.5 T. The spin magnetic moment of V (upper right panel) has been corrected using a correction factor ( $= 0.5 \pm 0.1$ ) which has been deduced by a linear extrapolation value from the reported values for heavier transition-metal ions [6].

- [4] B. T. Thole, P. Carra, F. Sette, and G. van der Laan, *Phys. Rev. Lett.* **68**, 1943 (1992).
- [5] P. Carra, B. T. Thole, M. Altarelli, and X. Wang, *Phys. Rev. Lett.* **70**, 694 (1993).
- [6] Y. Teramura, A. Tanaka, and T. Jo, *J. Phys. Soc. Jpn.* **65**, 1053 (1996).

\* nonaka@wyvern.phys.s.u-tokyo.ac.jp